International Journal of Rock Mechanics & Mining Sciences 128 (2020) 104244

Contents lists available at ScienceDirect

International Journal of Rock Mechanics and Mining Sciences

journal homepage: http://www.elsevier.com/locate/ijrmms

An experimental study of a novel liquid carbon dioxide rock-breaking technology

Qi-Yue Li [a], Guan Chen [b,*], Da-You Luo [a,c,**], Hai-Peng Ma [d], Yong Liu [b]

[a] School of Resource and Safety Engineering, Central South University, 932 South Lushan Road, Changsha, 410083, PR China
[b] State Key Laboratory of Water Resources and Hydropower Engineering Science, Institute of Engineering Risk and Disaster Prevention, Wuhan University, 299 Bayi Road, Wuhan, 430072, PR China
[c] Department of Civil and Environmental Engineering, Francis College of Engineering, University of Massachusetts Lowell, 1 University Avenue, Lowell, 01854, USA
[d] Junkai Non-explosives Blasting Sci&Tec, Kaifu District, Changsha, 410005, PR China

ARTICLE INFO

Keywords:
Liquid carbon dioxide
Rock breaking
Non-explosive technique
Vibration
Shock pressure

ABSTRACT

Safely and high-efficiently breaking rock is of practical significance. In some engineering, explosive blasting may be restricted for its side effects. Traditional non-explosive methods like demolition agent and rock breaking machine are generally time-consuming. Therefore, this study proposes a novel liquid carbon dioxide rock-breaking technology and designs the relative device. The effectiveness, safety and high-efficiency of the proposed technology are investigated by shock pressure test, vibration site test and field rock breaking experiment. The experimental results show that the duration of the monitoring shock pressure is around 1500 μs. The shock pressure signal of liquid carbon dioxide tube breaking in free condition contains four stages, namely, increasing exponentially, decreasing oscillatory, stabilization, and negative pressure stage. As pressure sensor is set at 850 mm from the test tube radially, the shock pressure monitored increases to the maximum value of 115.7 kPa within 6 μs. During the liquid carbon dioxide rock breaking, the vertical component of the peak particle velocity of vibration is 173 mm/s, 85 mm/s and 35 mm/s along distance at 1.5 m, 2.5 m and 3.5 m from the tube, respectively. The Fourier power spectra results show that about 85% energy distributes at 6–60 Hz. The vibration caused by the novel technology can meet the requirement of mainstream blasting safety criteria better than that of explosive blasting. Finally, the technology is successfully applied in rock excavation at a metro station construction site. The proposed liquid carbon dioxide rock-breaking technology is preliminarily demonstrated to be safer than explosive blasting and more efficient than traditional non-explosive techniques.

1. Introduction

Safely and efficiently breaking rock is significant in municipal, mining and hydropower engineering. Explosive blasting is generally deemed as the most effective rock breaking technique for its advantages on economic and high-efficient. However, owing to its side effects (e.g. blasting vibration, noxious gases, flames and flying rocks), explosive blasting may be restricted in some engineering, such as coal mine[1] and metro construction being adjacent to urban resident areas.[2] Hence, to meet the requirement of safety, non-explosive rock breaking techniques like demolition agent and rock breaking machine are usually applied as substitute of explosive. These techniques are quite safe, but time-consuming. Therefore, this study aims to propose a novel rock breaking technology which is safer than explosive blasting and more efficient than traditional non-explosive techniques.

Inspired by Cardox systems, a novel liquid carbon dioxide rock breaking technology is proposed. Cardox system is a carbon dioxide gas expansion fracturing technology. In 1990s, Singh simply described a rock breaking project with Cardox system at quarrying in Turkey.[3] However, except an application of Cardox system in enhancing gas drainage efficiency in coal mine performed in China in 2015,[4] few studies on Cardox system are conducted recently. Although it is time-consuming, the Cardox system provides a novel idea in rock breaking, i.e. breaking rock with liquid carbon dioxide. To investigate its feasibility, the relative references are reviewed and summarized at Table 1. Currently, many researches focus on liquid/supercritical carbon

* Corresponding author.
** Corresponding author. School of Resource and Safety Engineering, Central South University, 932 South Lushan Road, Changsha, 410083, PR China
E-mail addresses: chenguan@whu.edu.cn (G. Chen), Dayou_Luo@student.uml.edu (D.-Y. Luo).

https://doi.org/10.1016/j.ijrmms.2020.104244
Received 13 July 2019; Received in revised form 6 February 2020; Accepted 6 February 2020
Available online 25 February 2020
1365-1609/

Table 1
Summary of researches on carbon dioxide breaking rock.

Year	Reference	Objects	Methods	Remarks
2019	Sampath et al.[5]	L-CO_2 fracturing	Experiment with coal	Fracturing process and fracture network characteristics in various rank coal samples
2019; 2018	Wang et al.[6]; Yang et al.[7]	SC-CO_2 fracturing	Theoretical model and experimental/ numerical verification	Proposed a temperature and pressure field calculating model
2019	Wang et al.[8]	SC-CO_2 fracturing	Finite element-discrete simulation	Proposed an adaptive simulation method and analyzed the micro-seismic model of horizontal wells
2019	Zhou et al.[9]	SC-CO_2 fracturing	Experiment with concrete	Effects of temperature on fracturing
2018	Cai et al.[10]	SC-CO_2 fracturing	Experiment with organic glasses	Discussing the mechanism of SC-CO_2 fracturing based test results
2018	Deng et al.[11]	L-CO_2 fracturing	Comparison experiment on L-CO_2 and water with shale and coal	The L-CO_2 better than water as fracturing fluid due to its lower viscosity
2018	Gao et al.[12]	L-CO_2 breaking rock	Theoretical analysis and experiment	Proposed a formula for calculating crack propagation radius
2018	Hu et al.[13]	L-CO_2 increasing permeability	Numerical simulation and field experiment	Analyzing the fracture propagation pattern in coal seams and the effectiveness of L-CO_2 in increasing the permeability
2018	Li et al.[14]	L-CO_2 fracturing	Experiment with tight sandstone	The dynamic filtration behavior of L-CO_2 and its influence factors
2018	Zhao et al.[15]	SC-CO_2 fracturing	Experiment with shale	Observing the fracture propagation
2017	Cao et al.[16]	L-CO_2 increasing permeability	Experiment in Luan mine	Statistic of the permeability enhancement result and discussed the fracture initiation mechanism
2017	Chen et al.[17]	L-CO_2 increasing permeability	Simulation analysis and filed investigation	The influence scope and permeability enhancement results
2017	Song et al.[18]	SC-CO_2 fracturing	Theoretical modeling	Pressure transmission characteristics and its influence factors in the tubing (pressure transmission is correlated with fracturing results)
2017	Zhang et al.[19]	SC-CO_2 fracturing	Comparison experiment on L-CO_2 and water with shale	L-CO_2 require 50% less pressure for initiation fractures and increasing fracturing conductivity
2015	Bennour et al.[20]	L-CO_2 fracturing	Comparison experiment on viscous oil, water and L-CO_2 with shale	Comparing different fracture Model of three fracturing fluid and the advantages of L-CO_2 in inducing more extending cracks with many branches with Model II being dominant.
2015	He et al.[21]	SC-CO_2 fracturing	Numerical simulations and experiment	Pressurization effect of SC-CO_2 compared with water fracturing on fracturing and its influence factors
2015	Wang et al.[22]	SC-CO_2 breaking rock	Experiment with concrete	Analyzing the six main influence factors on rock-breaking by SC-CO_2
2013	Van et al.[23]	L-CO_2 storage	CO_2 explosive experiment	Analyzing the effects of temperatures on CO_2 storage and the proposed a critical explosive temperature of CO_2 cylinders
2012	Ishida et al.[24]	SC-CO_2 and L-CO_2 fracturing	Experiment with granite	Cracks extending more three dimensionally by SC-CO_2 compared with L-CO_2, and both SC- and L-CO_2 require lower breakdown pressure than water
2012	Perera et al.[25]	Injecting CO_2 increasing permeability	Experiment with coal and numerical simulation	Coal permeability enhancement in higher injection pressures at limited temperature ranges; discussing the adsorption based swelling phenomena of CO_2 by comparing with N_2

Note: L-CO_2 – liquid carbon dioxide; SC-CO_2 – supercritical carbon dioxide (phase diagram of CO_2 see Wang et al.[8]).

dioxide fracturing, few about directly breaking rock. Especially, it is applied in two engineering fields, namely, hydraulic fracturing substituting water as hydraulic liquid and increasing permeability of coal seam. The liquid carbon dioxide fracturing initiation and fracturing propagation characteristics are studied theoretically and experimentally. The influence factors like temperatures on fracturing are also analyzed. These investigations show that the advantages of liquid/-supercritical carbon dioxide include lower environmental impact,[5] heat transfer promoting branched and cross fractures,[9] reducing 50% pressure for initiate fractures and increasing fracture conductivity[19] and adsorption based swelling phenomena.[25] Although there are still some challenges, both the liquid and supercritical carbon dioxide show high potential in rock breaking.[26]

A novel liquid carbon dioxide rock-breaking technology is proposed. The liquid carbon dioxide rock-breaking tube is designed firstly. Then, the effectiveness, safety and high-efficiency of the proposed technology are verified using three experiments; that is shock pressure test, vibration site test and field rock breaking experiment. As one of the most

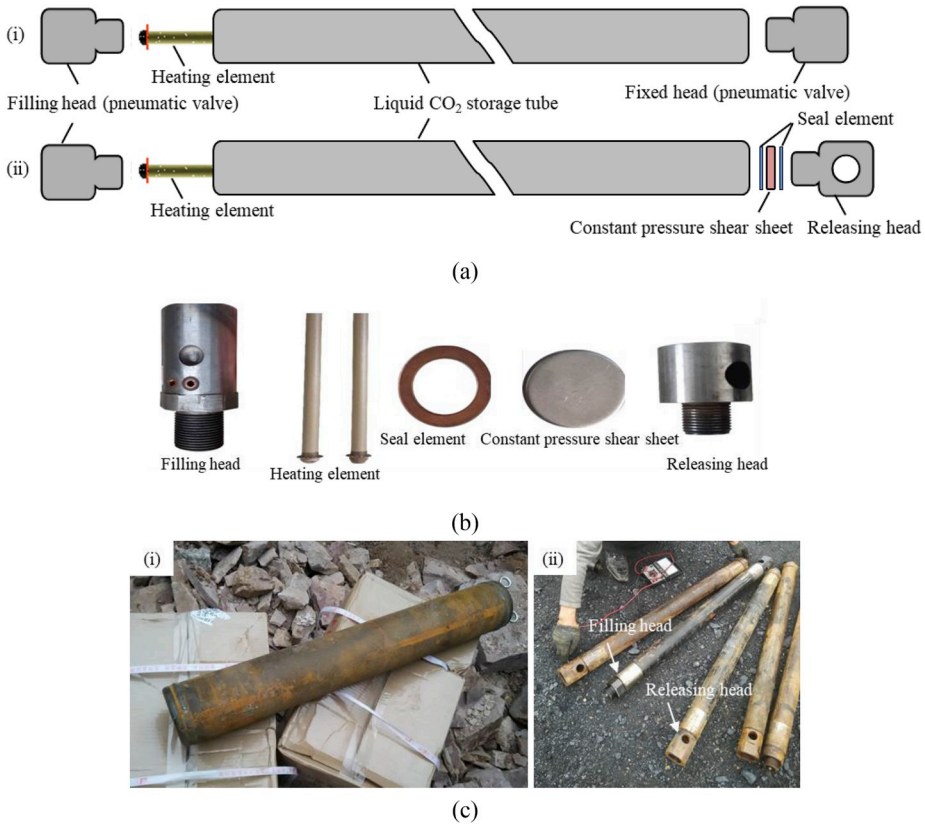

Fig. 1. The liquid carbon dioxide rock breaking tubes. (a) Structural diagram, (i) disposable tube, (ii) non-disposable tube; (b) parts drawing; (c) real product, (i) disposable tube, (ii) non-disposable tube.

significant vice effects on rock breaking,[27] the vibrations are analyzed in both time and Fourier frequency domain. In addition, the advantages and limitations of liquid carbon dioxide technology are discussed as well. The results indicate that the liquid carbon dioxide rock-breaking technology is prior to explosive blasting and traditional non-explosive techniques, especially in some vulnerable areas.

2. Liquid carbon dioxide rock-breaking tube

To meet the requirements of different engineering conditions, the disposable and non-disposable liquid carbon dioxide rock breaking tubes are designed as shown in Fig. 1. The technique parameters of these two tubes are listed as follows. Regarding to materials, the disposable and non-disposable tube are made of Q235 steel (refers to Chinese National Standard - Carbon Structural Steels GB/T 700–2006) and 20# steel (refers to Quality Carbon Structural Steels GB/T 699–2015), respectively. Based on shell theories, the ratio of inner and outer diameter of the disposable and non-disposable tube is designed as about 1.10 and 1.55, respectively. In this study, the dimension of the disposable and non-disposable tube is 1000 mm × 77 mm × 89 mm and 1200 mm × 47 mm × 73 mm (length × inner diameter × outer diameter), respectively, which can store 3.8 kg and 1.6 kg liquid carbon dioxide in general, respectively.

Owing to the difference in materials, structures, tube sizes and carbon dioxide storage capacities, these two tubes also vary in gas releasing way, application ranges and rock-breaking effects. The non-disposable tube releases the carbon dioxide from a certain vent rather than breaking the whole tube as the disposable tube. Environmental protection is the priority consideration in designing the non-disposable tube as it is recyclable. However, its installation and recycling process is time-consuming, and it is unlikely to be recycled in some cases limited by the geological and construction conditions. Thereafter, the disposable tube is designed. It is relatively expensive but more efficient. Therefore, the disposable tube has better applicability compared with the non-disposable tube that is commonly applied in engineering sites where the installations and recycles are convenient. Generally, the rock-breaking effect and vibration amplitudes are closer relative with the dioxide carbon mass than the types of the tubes. However, further studies need to carry out to investigate the influencing factors on rock-breaking effects and vibration amplitudes.

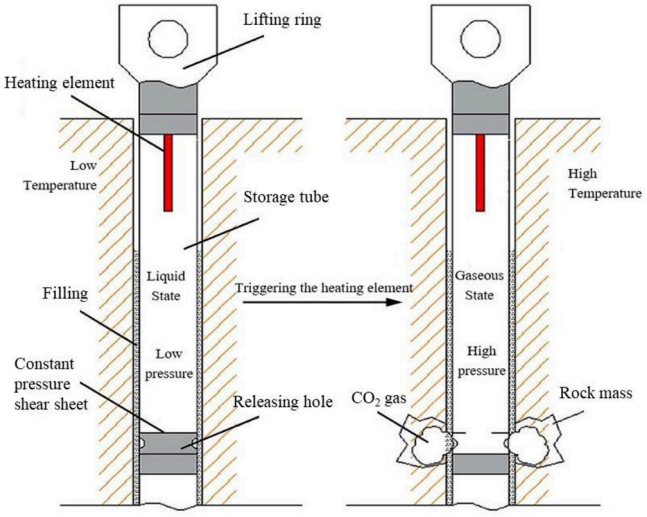

Fig. 2. Work principle diagram of liquid carbon dioxide rock breaking technology.

Although these two tubes have various diversities, they work

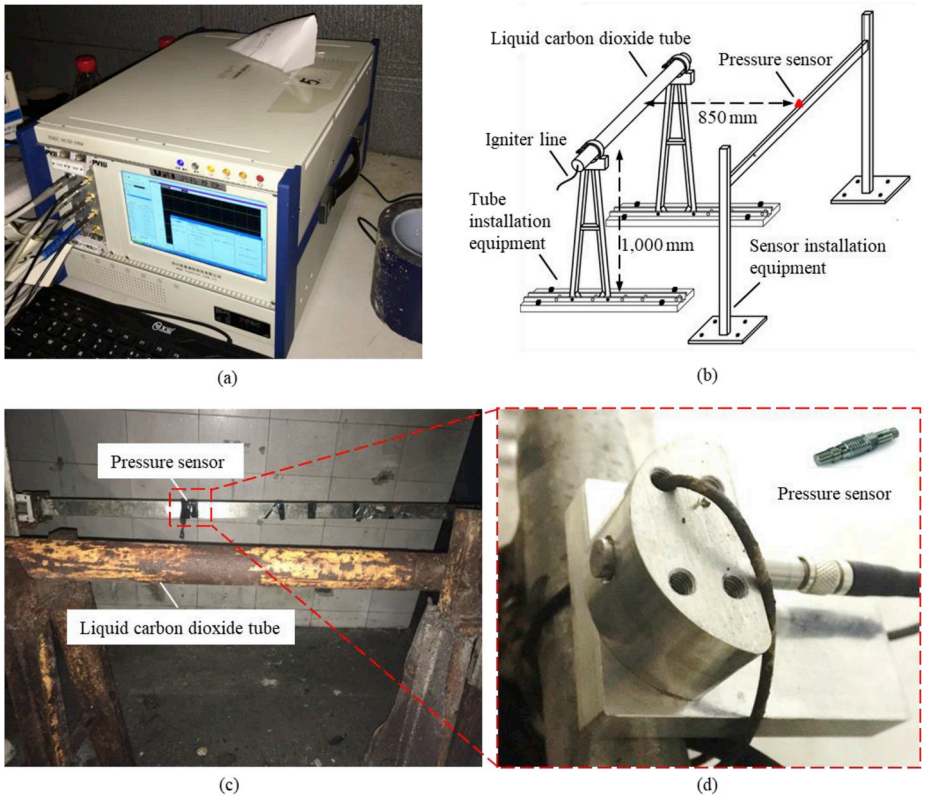

Fig. 3. Shock pressure test system. (a) NUXI-1004 dynamic test analyzer; (b) shock pressure test system and parameters; (c) scene of shock pressure test system; (d) pressure sensor installation.

similarly in principle. However, the rock-breaking mechanism of the liquid carbon dioxide technology is a complex coupling problem. It involves rock dynamics, fracture mechanics, stress wave propagation, thermodynamics and fluid mechanics etc.[28–30] Hence, this study only preliminarily describes the rock-breaking process. Liquid carbon dioxide rock-breaking is a pure physical process, which breaks rocks by the instantaneous release of large quantities of gaseous carbon dioxide. The rock breaking principle diagram of non-disposable liquid carbon dioxide tube is shown as Fig. 2. The heating element is triggered by the electric initiation device; subsequently the stored liquid carbon dioxide is activated, and transforms to a supercritical state. Then, the inner pressure rapidly rises to exceeding the constant stress shearing sheet maximum shear strength (regarding to the disposable tube, the inner pressure rapidly rises to exceed the maximum shear strength of the tube). Simultaneously, the gas carbon dioxide is released outward from the broken constant stress shearing sheet immediately. The rocks can be broken effectively combined the effects of strain wave and air-wedge.[31]

3. Experiments

3.1. Shock pressure laboratory test

3.1.1. Test apparatus and procedures

To measure the shock pressure of liquid carbon dioxide phase changing in rock breaking technology, a NUXI-1004 dynamic test analyzer and the pressure sensor (PCB113A24) were used, shown in Fig. 3 (a) and (d), respectively. The maximal measure pressure of NUXI-1004 dynamic test analyzer is 600 MPa; the sample frequency is 10 MHz. The range of the pressure sensor is 0–6.895MPa, with the sensitivity of 0.73 mV/kPa, the operating temperature of −20–85 °C, resolution of 0.035 kPa, and high linearity of ±1%. A disposable liquid carbon dioxide tube is applied (its technical parameters are mentioned above) in the test. The installation equipment was designed under free field conditions for monitoring the shock pressure. The pressure sensor is tied in the beam. The layouts of liquid carbon dioxide tube and the pressure sensor are shown in Fig. 3(b) and (c).

The test procedures elaborate as following: (a) installing the experimental structure, and ensuring the liquid carbon dioxide tube is 1 m in height from the ground; (b) assembling the pressure sensor, certifying it at the same height of the tube, and vertical to the tube; (c) debugging the NUXI-1004 dynamic test analyzer; (d) activating the liquid carbon dioxide with the heating element; (e) obtaining the experimental data.

3.1.2. Test results

The shock pressure test results show that the disposable liquid carbon dioxide tube is broken to several fragments, as shown in Fig. 4(a). It certifies the design rationality of the disposable tube. The shock pressure signal (see Fig. 4(b)) shows that its duration is around 1500 μs; the peak shock pressure is 115.7 kPa; and the minimum negative pressure is −17.89 kPa. Overall, the shock pressure of phase changing show a form of planar Friedlander wave.[32] It increases exponentially first; subsequently, it turns to be oscillatory decreasing. Moreover, the rate of increasing is much higher than decreasing. Finally, there appears a period of negative pressure before disappearing.

3.2. Vibration site test

3.2.1. Vibration monitoring

Vibration is one of the most main vice effects in rock breaking engineering construction. The rock breaking vibration test is carried out to evaluate the vibration level. The arrangements and related parameters of the liquid carbon dioxide tubes and the vibration monitoring device are shown in Fig. 5. Owing to the limitations of site conditions, the monitoring sensors were installed closely to the reinforcement wall, which may affect the monitoring results by reflecting the vibration waves. However, the depth of the reinforcement wall was substantially

(a)

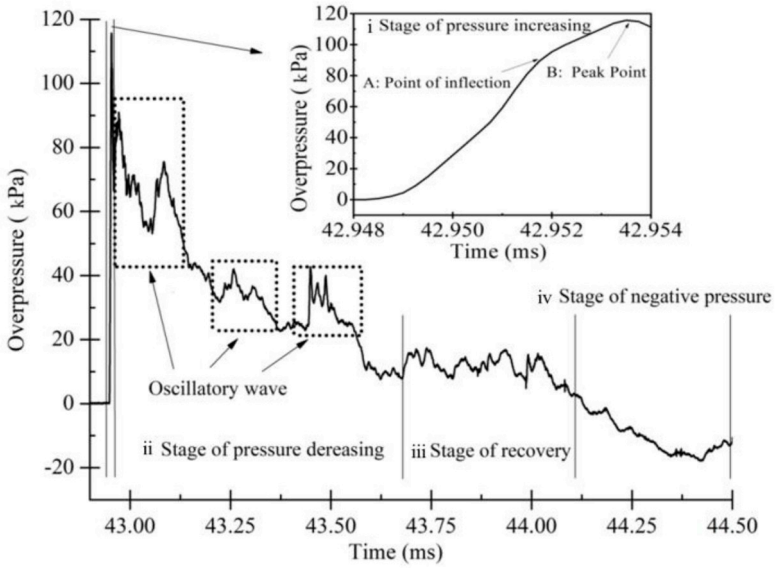

(b)

Fig. 4. Shock pressure test results. (a) The breaking disposable liquid carbon dioxide tube; (b) monitoring shock pressure signal.

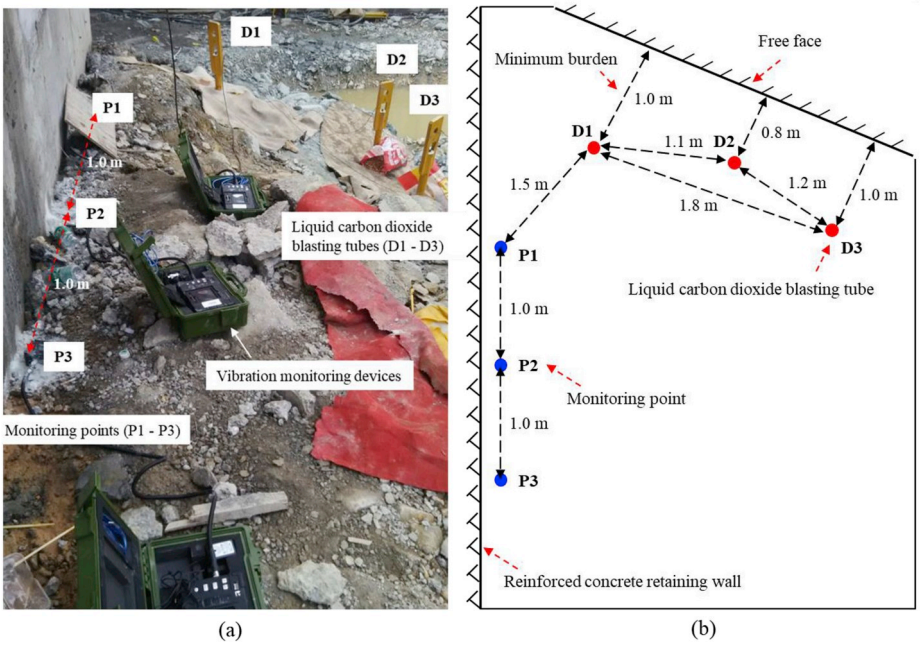

(a) (b)

Fig. 5. Arrangements and related parameters of liquid carbon dioxide tube and vibration monitoring devices. (a) Site layout; (b) layout parameters sketch.

equal to installation level of the vibration monitoring sensors. Therefore, the effects of reinforcement wall on vibration monitoring results were not taken into account in this study. The non-disposable liquid carbon dioxide tubes are applied. The shear strength of constant pressure shear sheet is 184–222 MPa, and the weight of liquid carbon dioxide of a single tube is 1.6 kg. NUBOX-8016 vibration monitoring devices are used in vibration monitoring (see Fig. 5). NUBOX-8016 can connect one three-way detector, with 0.0047 cm/s in the minimum trigger level, 0.1 cm/s to 33 cm/s in the velocity range, 5000 Hz in the fixed sampling frequency and 4.5 Hz–300 Hz in its frequency response range. In addition,

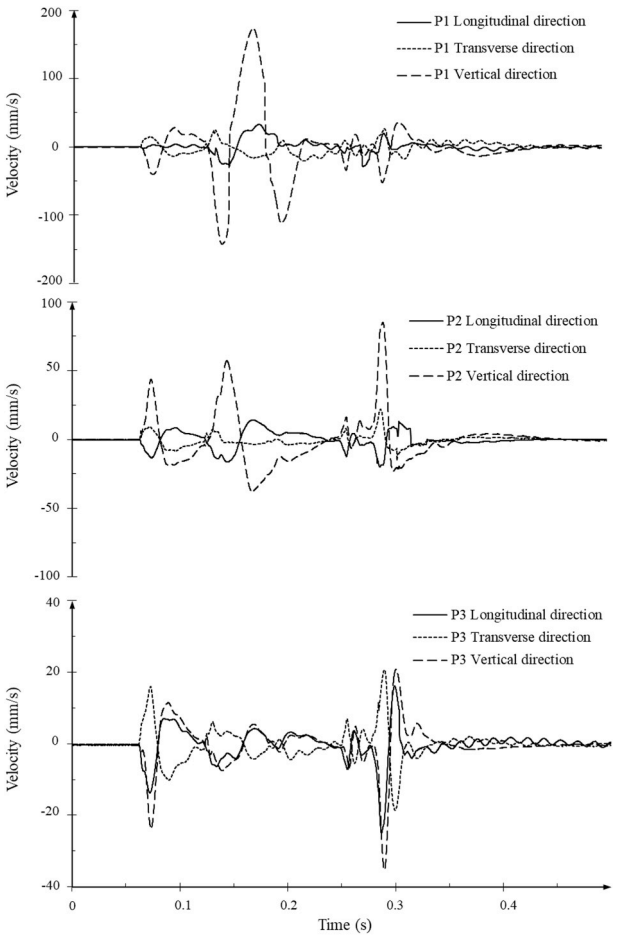

Fig. 6. Vibration monitoring signals (P1, P2, P3 representing vibration monitoring points).

the diameter and length of borehole is 90 mm and 3000 mm, respectively. A borehole installs two liquid carbon dioxide tubes in series, i.e. 3.2 kg liquid carbon dioxide charged in each borehole. The interspace between the liquid carbon dioxide tube and borehole is filled by fine sands.

3.2.2. Vibration signals

The monitoring vibration signals show that the vibration velocity of vertical direction is higher than longitudinal and transverse direction in general (see Fig. 6). The waveform and vibration velocity of longitudinal and transverse direction signals are basically the same. However, as the distances increasing, the vertical direction vibration velocities significantly attenuate, and three directions trend to be the same. The peak particle velocity in vertical direction of P1 (vibration monitoring point 1), P2 and P3 is 173 mm/s, 85 mm/s and 35 mm/s respectively. The vibration duration is around 0.3 s. Because of waveform overlay, the waveform exits a second peak before attenuating to zero.

3.3. Field rock breaking experiment

3.3.1. Background

Hunan University Metro Station is in Changsha, China, and surrounded by brick structures and reinforced concrete structure buildings. The distance between the station construction site and the nearest brick building is around 17 m, shown in Fig. 7. The geology of excavation range is mainly composed with two strata: the upper clay soil around 3–6 m; the lower bedrocks with different degree of weathering slate. The Protodyakonov coefficient of slate rocks is $f = 5–8$. The traditional rock

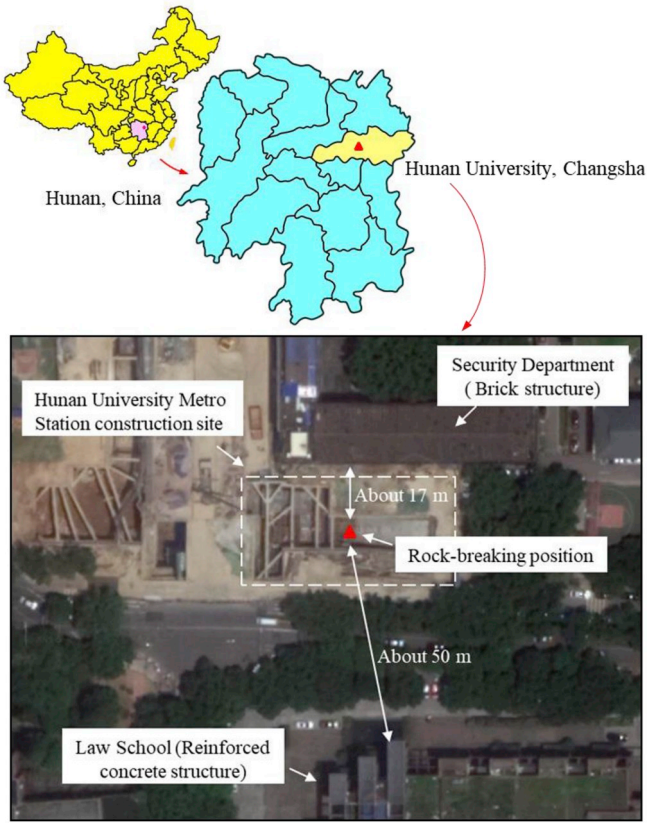

Fig. 7. Location and surroundings of Hunan University Metro Station.

breaking machine is unable to excavate the slate rocks effectively. Moreover, because the station is near to the residential and educational communities, the explosive blasting is strictly limited by government in this construction site. Hence, the proposed liquid carbon dioxide rock breaking technology is implemented.

The station construction site and arrangements of liquid carbon dioxide tubes (non-disposable) are shown in Fig. 8(a) and (b), respectively. The drilling hole is 90 mm and 3000 mm in diameter and length, respectively. Two liquid carbon dioxide tubes are installed in each drilling hole, i.e. 3.2 kg liquid carbon dioxide in each borehole. The interspace between the liquid carbon dioxide tube and borehole is filled by fine sands. Four non-disposable liquid carbon dioxide tubes in two drilling holes were detonated simultaneously.

3.3.2. Rock breaking effects

The rock breaking process is shown in Fig. 9. Stage 1 represents the initial status of the excavation face. The rock mass is fractured into several rocks by air-wedge effects in Stage 2. Combined the effects of shock wave and air-wedge, the rocks are broken into fragments and throw out in Stage 3 and 4. The excavation face after rock breaking is described in Stage 5. About 20 m^3 of rocks are excavated by four liquid carbon dioxide tubes, i.e. 6.4 kg liquid carbon dioxide. The liquid carbon dioxide unit consumption is 0.32 kg/m^3. The rock fragmentation degree meets the requirements of transportation. The noise caused by liquid carbon dioxide rock breaking is lower than 76 dB at 16 m away.

4. Results and discussions

4.1. Shock pressure characteristics

The shock pressure signal shows a typical form of a planar Friedlander wave,[32] which can be readily divided into four main stages, namely, increasing exponentially, decreasing oscillatory, stabilization,

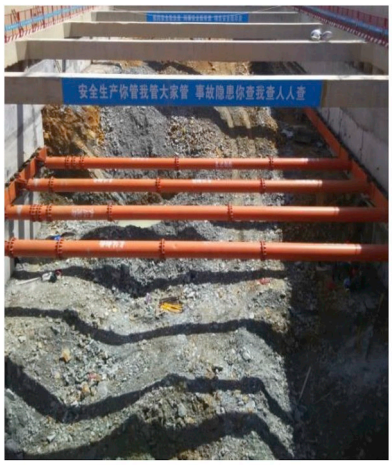

(a)

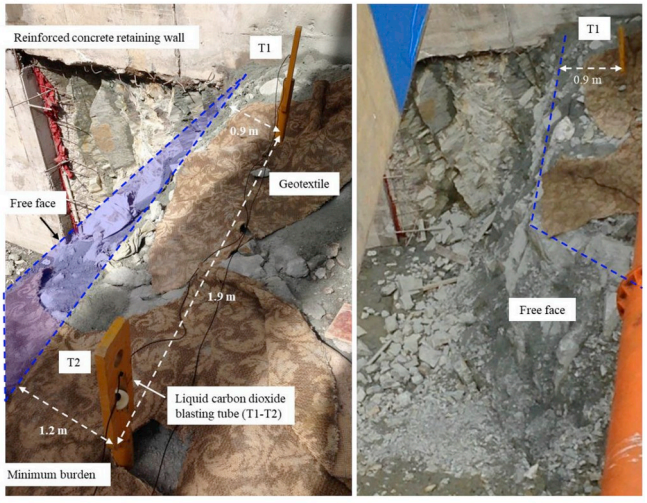

(b)

Fig. 8. Engineering site condition. (a) Metro station construction foundation pit; (b) arrangements and parameters of liquid carbon dioxide tubes.

and negative pressure stage (see Fig. 4(b)). During the first stage, the shock pressure rapidly increases to the maximum value of 115.7 kPa within 6 μs. In addition, there is an inflection point during the increasing stage, as point A in Fig. 4(b). The shock pressure increases rapidly before point A; then the speed slows down slightly until it reached the maximum value, as point B in Fig. 4(b). It may be attributed to the decreases of the amount of gas carbon dioxide after point A. In the second stage, the shock pressure deceases from 115.7 kPa to 10 kPa within around 750 μs. The shock pressure decreased in an oscillatory way with three distinct oscillatory waves, which is mainly caused by the shaking of sensor installation equipment. In the third stage, although the fluctuations still consist, the shock pressure signal basically keeps stability at around 10 kPa. In the fourth stage, the pressure sensor detected a negative pressure, which is caused by effects of the shock pressure and ambient pressure. As the compressed air caused by the overpressure wave is away from the sensor, a thin air zone would exist around the pressure sensor temporally, thus resulting in a negative ambient pressure zone.

4.2. Vibration signal spectrum characteristics

According to the blasting safety criteria,[33] both time and frequency domain characteristics of vibration signal are critical in safety analysis. The time domain characteristics have been analyzed in Section 3.2.2 preliminarily. Here, the discrete Fourier transform (DFT) was conducted to investigate the frequency domain characteristics further. DFT is an effective tool for spectrum analysis and widely applied in engineering signal processing field.[34]

For signal $S(n)$ ($n = 0, 1, 2, \ldots, N\text{-}1$), its DFT can be expressed as Eq. (1).

$$f_k = \sum_{n=0}^{N-1} S(n) e^{-i\frac{2\pi}{N}kn}, k = 0, 1, \ldots, N-1 \quad (1)$$

where f_k ($k = 0, 1, 2, \ldots, N\text{-}1$) is the DFT coefficients. From the perspective of signal processing, the DFT coefficient represents amplitude of corresponding frequency. The Fourier frequency range depends on sample frequency f_s. In this study, the sample frequency of vibration monitoring device is 5000 Hz. Based on sampling theory, its Nyquist frequency $N_f = 2500$ Hz, i.e. Fourier frequency range is 0–2500 Hz.

To analyze the spectrum characteristics, the Fourier power spectrum P_k ($k = 0, 1, 2, \ldots, N\text{-}1$) is calculated by Eq. (2).

$$P_k = f_k \overline{f_k}, k = 0, 1, \ldots, N-1 \quad (2)$$

where $\overline{f_k}$ is the complex conjugate of f_k. Based on Eq. (2), the power spectra of monitored vibration signals are calculated (see Fig. 10).

To analyze the energy distribution characteristics in frequency domain, the normalized cumulative power spectrum C_m ($m = 0, 1, 2, \ldots, N\text{-}1$) of vibration signals is also calculated by Eq. (3) (see Fig. 11).

$$C_m = \frac{\sum_{k=0}^{m} P_k}{\sum_{k=0}^{N-1} P_k}, m = 0, 1, 2, \ldots, N-1 \quad (3)$$

Figs. 10 and 11 show that the dominant frequency of P1, P2 and P3 in vertical direction is 15 Hz, 13 Hz and 13 Hz, respectively. Energies in vertical direction are much higher than longitudinal and transverse direction in P1. However, with the increasing of distance, the energies in three directions trend to be equal. About 85% energy distributes on 6–60 Hz. With the increase of distance, the energies attenuate faster, but distribute tighter, specifically, energies gradually moving from 0 to 10

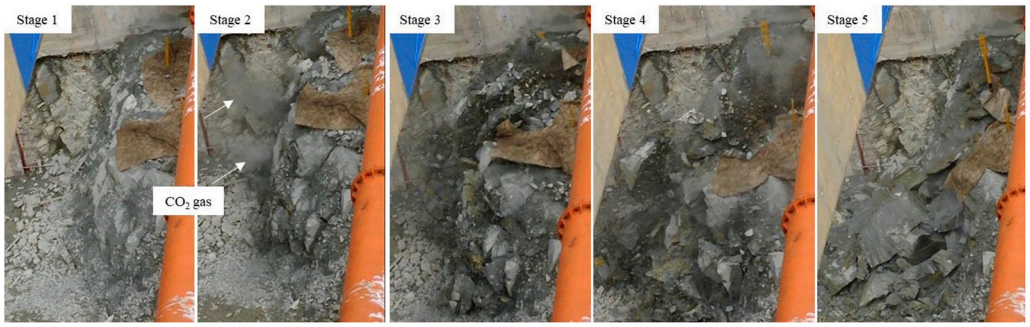

Fig. 9. Rock breaking process by liquid carbon dioxide technology.

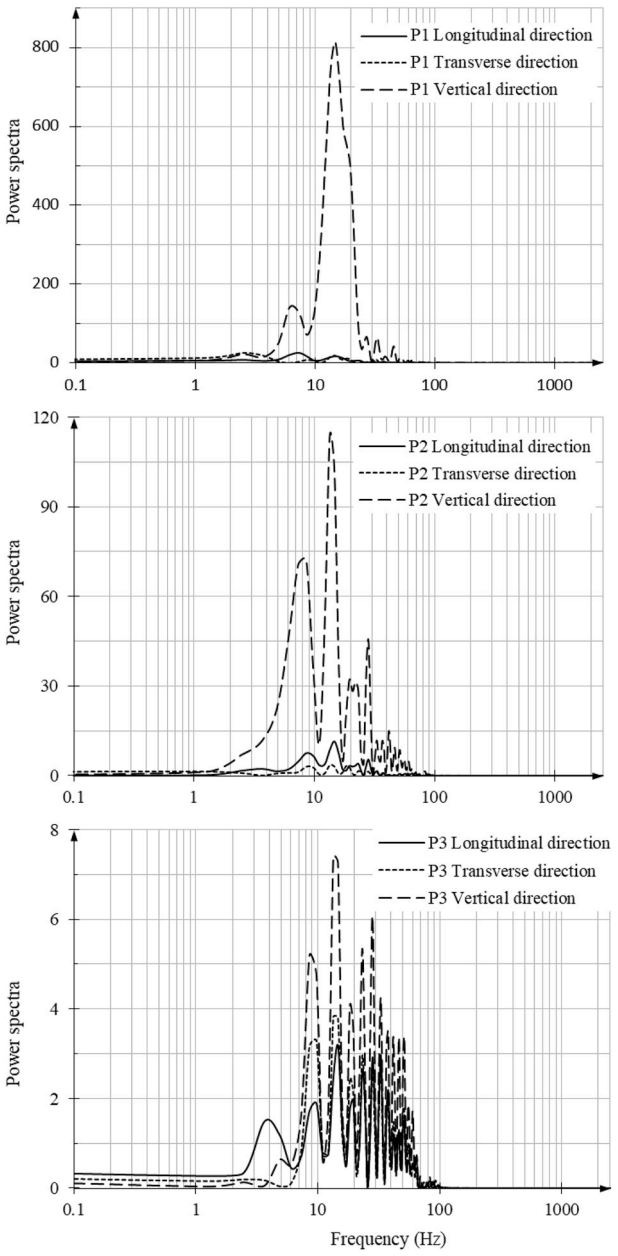

Fig. 10. Fourier power spectra of vibration signals (P1, P2, P3 representing vibration monitoring points).

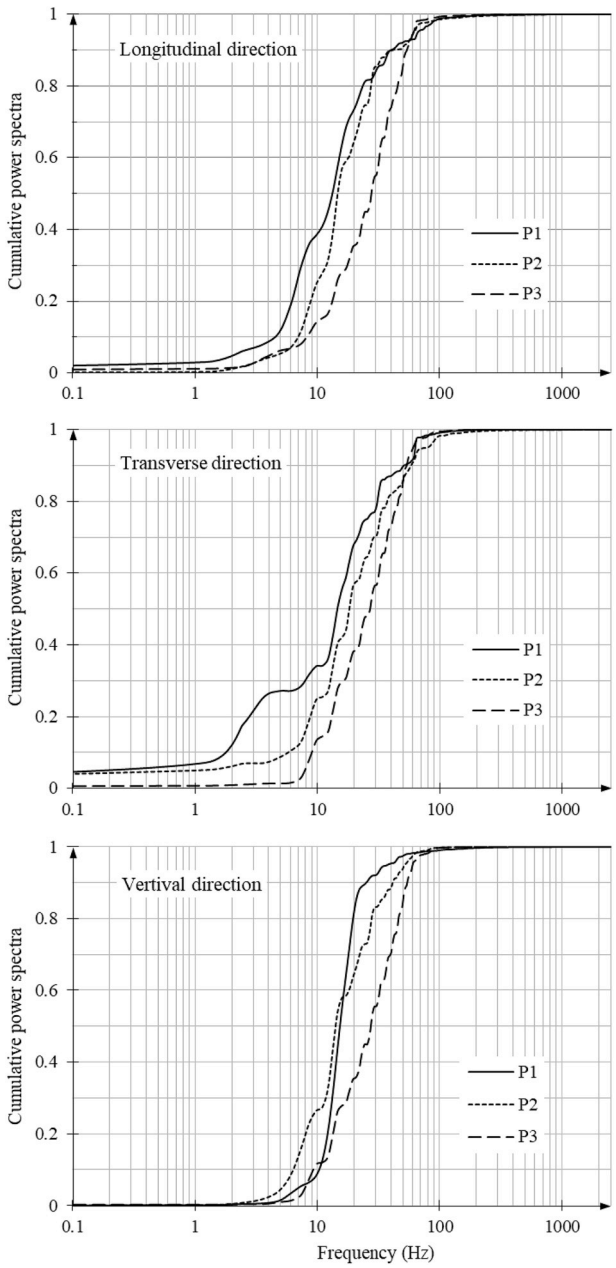

Fig. 11. Normalized cumulative power spectrum of vibration signals (P1, P2, P3 representing vibration monitoring points).

Hz to 10–60 Hz regions.

4.3. Advantages and limitations

The vibration site experimental results show that the vibration frequency is about 6–60 Hz; the velocity is about 35 mm/s at around 5 m from the blasting center, which can meet the safety requirements of mainstream blasting safety criteria.[33] Due to the lower vibration level, the liquid carbon dioxide technology is prior to explosive blasting in the fields like urban residential area and other vibration strictly controlled areas. Moreover, both the liquid carbon dioxide weights and the location of vent are controllable for non-disposable tube; that is the bursting strength and main energy release direction can be controlled. Therefore, the liquid carbon dioxide technology could achieve fine control blasting and improve the reliability in rock breaking. In addition, the liquid carbon dioxide technology is a physical explosion by liquid carbon dioxide phase changing without flame and chemical noxious gases. Hence, it can be used in the fields with non-flame and poor ventilation, such as improving coal seam gas drainage and excavated in high gas mine.

The efficiency and cost are analyzed based on the field experiment. The whole rock breaking processes cost about 1 h. A small-scale hydraulic rock drill is used in this study, which drilling velocity is about 0.5 m/min, and takes about 20 min. The transportations and installations of non-disposable tubes cost about 40 min. The unit consumption of liquid carbon dioxide is 0.32 kg/m^3. However, the rock-breaking efficiency could be affected by the site geological properties, such as Protodyakonov coefficient and geological discontinuities. The Protodyakonov coefficient could affect the rock fragmentation degree, and the air-wedge effect is closely related to the geological discontinuities (e.g. joints and fractures). The air-wedge effects may decrease in rock breaking processes as the fissure sufficiently developed, thus decreasing the rock breaking efficiency. Moreover, limited by the sizes of tube, the borehole utilization ratio is lower than explosive blasting. Although the installations process is more complex than explosive, the

transport control of liquid carbon dioxide tubes is less strict. In addition, compared with traditional non-explosive techniques, the efficiency has been improved predominately using the proposed technique. The main cost of liquid carbon dioxide tube is the heating element. Generally, liquid carbon dioxide technology costs higher than explosive blasting at the same rock breaking volumes. However, with respect to traditional non-explosive rock breaking method, liquid carbon dioxide technology is economical overall.

Therefore, it is preliminarily validated that the liquid carbon dioxide rock-breaking technology is safer than explosive blasting and more economical and efficient than traditional non-explosive techniques. According to the statistics of China Association of Metros (CAMET), 5494.9 km urban metros in thirty-six cities have been built in China until Dec. 2018, and the investments are still growing. Ensuring safety and high-efficiency in urban metros construction are critical in China. Attributed to the advantages, the liquid carbon dioxide rock breaking technology has great opportunities.

5. Conclusions

This study proposed a novel liquid carbon dioxide rock-breaking technology. It has great advantages on less vibration, non-flame and non-noxious gases than explosive blasting, and more economic and high-efficient than traditional non-explosive techniques. As pressure sensor is setup at around 850 mm from the test tube, the peak shock pressure is 115.7 kPa. At 1.5 m, 2.5 m and 3.5 m from the breaking center, the vertical component of peak particle velocity is 173 mm/s, 85 mm/s and 35 mm/s, respectively. The Fourier dominant frequency of vibration is from 13–15 Hz, and almost 85% energy distributes from 6–60 Hz. The vibration level induced by proposed technology can meet the requirement of blasting safety criteria better than explosive blasting. Moreover, the liquid carbon dioxide technology is successfully applied in rock excavation at a metro station construction site, and its effectiveness, safety and high-efficiency is preliminarily verified. However, the results are concluded based on limited experiments in this study. More tests with different types of rock and construction sites need to carry out to validate its universality.

The proposed liquid carbon dioxide rock-breaking technology may provide a great opportunity for non-explosive constructions. However, few studies on liquid carbon dioxide rock-breaking technology are found currently. Further investigations need to carry out, especially in the effects of rock properties on rock-breaking efficiency, the rock-breaking mechanism of liquid dioxide carbon technology and the inner pressure measuring of tube during rock breaking.

Acknowledgements

This research is supported by the National Key R&D Program of China (Grant No. 2016YFC0600802) and the National Natural Science Foundation of China (Grant No. 51879203).

References

1 Xu J, Zhai C, Qin L, Yu G. Evaluation research of the fracturing capacity of non-explosive expansion material applied to coal-seam roof rock. *Int J Rock Mech Min Sci*. 2017;94:103–111.
2 Shang J, Zhao Z, Aliyu MM. Stresses induced by a demolition agent in non-explosive rock fracturing. *Int J Rock Mech Min Sci*. 2018;107:172–180.
3 Singh SP. Non-explosive applications of the PCF concept for underground excavation. *Tunn Undergr Space Technol*. 1998;13(3):305–311.
4 Lu T, Wang Z, Yang H, Yuan P, Han Y, Sun X. Improvement of coal seam gas drainage by under-panel cross-strata stimulation using highly pressurized gas. *Int J Rock Mech Min Sci*. 2015;77:300–312.
5 Sampath KHSM, Perera MSA, Elsworth D, et al. Effect of coal maturity on CO_2-based hydraulic fracturing process in coal seam gas reservoirs. *Fuel*. 2019;236:179–189.
6 Wang J, Wang Z, Sun B, Gao Y, Wang X, Fu W. Optimization design of hydraulic parameters for supercritical CO_2 fracturing in unconventional gas reservoir. *Fuel*. 2019;235:795–809.
7 Yang ZZ, Yi LP, Li XG, Chen YT, Sun J. Model for calculating the wellbore temperature and pressure during supercritical carbon dioxide fracturing in a coalbed methane well. *J CO_2 Util*. 2018;26:602–611.
8 Wang Y, Ju Y, Chen J, Song J. Adaptive finite element–discrete element analysis for the multistage supercritical CO_2 fracturing and microseismic modelling of horizontal wells in tight reservoirs considering pre-existing fractures and thermal-hydro-mechanical coupling. *J Nat Gas Sci Eng*. 2019;61:251–269.
9 Zhou D, Zhang G, Prasad M, Wang P. The effects of temperature on supercritical CO_2 induced fracture: an experimental study. *Fuel*. 2019;247:126–134.
10 Cai C, Kang Y, Wang X, et al. Mechanism of supercritical carbon dioxide (SC-CO 2) hydro-jet fracturing. *J CO_2 Util*. 2018;26:575–587.
11 Deng B, Yin G, Li M, et al. Feature of fractures induced by hydrofracturing treatment using water and L-CO_2 as fracturing fluids in laboratory experiments. *Fuel*. 2018;226:35–46.
12 Gao F, Tang L, Zhou K, Zhang Y, Ke B. Mechanism analysis of liquid carbon dioxide phase transition for fracturing rock masses. *Energies*. 2018;11(11):2909.
13 Hu G, He W, Sun M. Enhancing coal seam gas using liquid CO_2 phase-transition blasting with cross-measure borehole. *J Nat Gas Sci Eng*. 2018;60:164–173.
14 Li B, Zheng C, Xu J, Lv Q, Shi D, Li Z. Experimental study on dynamic filtration behavior of liquid CO_2 in tight sandstone. *Fuel*. 2018;226:10–17.
15 Zhao Z, Li X, He J, Mao T, Zheng B, Li G. A laboratory investigation of fracture propagation induced by supercritical carbon dioxide fracturing in continental shale with interbeds. *J Petrol Sci Eng*. 2018;166:739–746.
16 Cao Y, Zhang J, Zhai H, Fu G, Tian L, Liu S. CO_2 gas fracturing: a novel reservoir stimulation technology in low permeability gassy coal seams. *Fuel*. 2017;203:197–207.
17 Chen H, Wang Z, Chen X, Chen X, Wang L. Increasing permeability of coal seams using the phase energy of liquid carbon dioxide. *J CO_2 Util*. 2017;19:112–119.
18 Song W, Ni H, Wang R, Sun B, Shen Z. Pressure transmission in the tubing of supercritical carbon dioxide fracturing. *J CO_2 Util*. 2017;21:467–472.
19 Zhang X, Lu Y, Tang J, Zhou Z, Liao Y. Experimental study on fracture initiation and propagation in shale using supercritical carbon dioxide fracturing. *Fuel*. 2017;190:370–378.
20 Bennour Z, Ishida T, Nagaya Y, et al. Crack extension in hydraulic fracturing of shale cores using viscous oil, water, and liquid carbon dioxide. *Rock Mech Rock Eng*. 2015;48(4):1463–1473.
21 He Z, Tian S, Li G, Wang H, Shen Z, Xu Z. The pressurization effect of jet fracturing using supercritical carbon dioxide. *J Nat Gas Sci Eng*. 2015;27:842–851.
22 Wang H, Li G, Shen Z, et al. Experiment on rock breaking with supercritical carbon dioxide jet. *J Petrol Sci Eng*. 2015;127:305–310.
23 van der Voort MM, van Wees RMM, Ham JM, et al. An experimental study on the temperature dependence of CO_2 explosive evaporation. *J Loss Prev Process Ind*. 2013;26(4):830–838.
24 Ishida T, Aoyagi K, Niwa T, et al. Acoustic emission monitoring of hydraulic fracturing laboratory experiment with supercritical and liquid CO_2. *Geophys Res Lett*. 2012;39(16).
25 Perera MSA, Ranjith PG, Choi SK, Airey D. Investigation of temperature effect on permeability of naturally fractured black coal for carbon dioxide movement: an experimental and numerical study. *Fuel*. 2012;94:596–605.
26 Middleton RS, Carey JW, Currier RP, et al. Shale gas and non-aqueous fracturing fluids: opportunities and challenges for supercritical CO_2. *Appl Energy*. 2015;147:500–509.
27 Chen G, Li QY, Li DQ, Wu ZY, Liu Y. Main frequency band of blast vibration signal based on wavelet packet transform. *Appl Math Model*. 2019;74:569–585.
28 Chen Y, Zhou C, Jing L. Modeling coupled THM processes of geological porous media with multiphase flow: theory and validation against laboratory and field scale experiments. *Comput Geotech*. 2009;36(8):1308–1329.
29 Atkinson BK. *Fracture Mechanics of Rock*. Amsterdam: Elsevier; 2015.
30 Li KQ, Li DQ, Liu Y. Meso-scale investigations on the effective thermal conductivity of multi-phase materials using the finite element method. *Int J Heat Mass Tran*. 2020;151:119383.
31 Donze FV, Bouchez J, Magnier SA. Modeling fractures in rock blasting. *Int J Rock Mech Min Sci*. 1997;34(8):1153–1163.
32 Geng J, Mander T, Baker Q. Blast wave clearing behavior for positive and negative phases. *J Loss Prev Process Ind*. 2015;37:143–151.
33 Roy MP, Singh PK, Sarim M, Shekhawat LS. Blast design and vibration control at an underground metal mine for the safety of surface structures. *Int J Rock Mech Min Sci*. 2016;83:107–115.
34 Wang ZW, Li XB, Peng K, Xie JF. Impact of blasting parameters on vibration signal spectrum: determination and statistical evidence. *Tunn Undergr Space Technol*. 2015;48:94–100.